

# Tracking Control of A Human Swing Leg Considering Self-Impact Joint Constraint by Feedback Linearization Method

Yousef Bazargan-Lari\* Mohammad Eghtesad\*\*  
Ahmadreza Khoogar\*\*\* Alireza Mohammad-Zadeh\*\*\*\*

\* *Department of Mechanical Engineering, Science and Research Branch, Islamic Azad University, Tehran, Iran. (e-mail: bazarganlari@iaushiraz.ac.ir).*

\*\* *School of Mechanical Engineering, Shiraz University, Shiraz, Iran. (e-mail: eghtesad@shirazu.ac.ir)*

\*\*\* *Department of Mechanical Engineering, Science and Research Branch, Islamic Azad University, Tehran, Iran. (e-mail: khoogar@yahoo.com)*

\*\*\*\* *School of Engineering, Grand Valley State University, USA. (e-mail: mohammaa@gvsu.edu)*

---

**Abstract:** Walking is one of the main human gaits of leg locomotion. Despite the simplicity with which humans appear to walk, this gait is inherently complex with highly nonlinear dynamics. Walking is made up of two distinct phases: single support phase (SSP) and double support phase (DSP). Since single support phase accounts for a much larger share in a walking gait cycle; it has been the most interesting topic of studies in this field. In SSP, one leg appears as the swing (moving) leg and the other one will be stationary or stance leg; the swing leg is usually modelled as a fixed double pendulum. The links of a double pendulum, in this case, will represent the thigh and shank of a human leg and its joints, hip and knee, will connect the upper body to thigh and then shank, respectively.

The main differences in this study, compared to the previous works, are assuming the double pendulum is movable and considering the joint self-impact constraint in double pendulum modeling at the knee joint. This constraint has an important role in realizing the practical characteristics of a swing leg; in other words, imposing this constraint necessitates that the shank link cannot assume the rotation angles which are greater than that of the thigh link. Therefore, prominent objective of this research is to propose a nonlinear model-based control method for a constrained (joint self-impact) movable double pendulum which models a more realistic swing leg. Due to complex nonlinear terms in dynamics equations of the joint self-impact swing leg, we propose to design the controller by taking advantage of the feedback linearization control method, which is a benchmark method for complex nonlinear systems.

To achieve this goal, the available data of normal human gait will be taken as the desired trajectories for the hip and knee joints and the origin of the double pendulum. The simulation results of applying the proposed method to the constrained double pendulum demonstrate that the swing leg tracks the normal human gait with a negligible and acceptable error.

*Keywords:* Leg locomotion, Self-impact joint constraint, Movable double pendulum, Feedback linearization, Single support phase, Swing leg.

---

## 1. INTRODUCTION

Human locomotion is the ability of human to move from one place to another. It is considered from three perspectives of walking, jogging, and running gaits. Walking is one of the main gaits of locomotion and happens more frequently than the other ones. It is defined as subsequent gait cycles; each walking gait cycle means the period from initial contact of one foot to the following initial contact of the same foot. Human locomotion has been an active research field of study for many years Zhang and Zhu (2006). Although the walking appear to be a simple exercise for

the human, this locomotion gait is inherently complex with highly nonlinear dynamics, Rose et al. (2006), and has received a particular attention in recent years.

Walking is made up of two main distinct phases: single support phase (SSP), during which the walking advances as an open kinematic chain; and double support phase (DSP), during which the walking appears as a closed kinematic loop. Since SSP assumes a much longer portion of the gait cycle; this phase has been the main focus of research study in this field, Ayyappa (1997).

In single support phase one leg acts as the swing (moving) leg and the other one will be stationary or stance

leg, Ayyappa (1997). A thorough review of the relevant literature reveals that the swing leg is frequently modelled as a fixed double pendulum, Huang et al. (2007); Goswami et al. (1997).

The body joints are the junctions of two or more system organs. The relative motion of some of these organs are restricted with respect to each other through the joint; we refer to this type of joints as self-impact joints. Joint self-impact phenomenon is a natural property of the body; considering this phenomenon in modeling of the body can exhibit a more realistic behavior of the system.

One particular and important example of this type of the joints is the knee joint. A careful observation of walking reveals that in a complete period of walking gait cycle, joint self-impact phenomenon happens between shank and thigh at knee joint in specific times. This means flexion and extension of a leg has a specific angle range. A detailed schematic of knee joint is depicted in Fig. 1 and the joint self-impact is shown in Fig. 2, when shank and thigh are aligned.

Recently, inclusion of joint self-impact phenomenon in system modeling has been studied by a number of researchers in the fields of dynamical systems and biomechanics. They have pointed out that this phenomenon should be considered as a constraint in the governing equations, Singh et al. (2008); Ono et al. (2000, 2001, 2004); Sangwan et al. (2004); Mukherjee et al. (2007); Huang et al. (2007). This is despite the fact that in most studies, modeling has been carried out ignoring these constraints, Cross (2011); Miller (2011); Couceiro et al. (2008, 2009, 2010, 2012).

In self-impact phenomenon, after the constraint is established (the constraint setting stage), the members may move together for some moments (the constrained motion stage). The importance of investigating this type of dynamical systems, in our case a movable double pendulum with joint self-impact constraint, is that the governing dynamical equations should be modified due to the system switch from the free motion state to a constrained one. Moreover, designing a controller for this modified system will be an interesting problem.

Due to discontinuity and nonlinearity of this phenomenon, controlling of this system becomes very complicated and will need advanced control methods; this has remained undiscussed in the literature and will be the main focus of this paper.

Many researches have been carried out for controlling the swing leg without considering this constraint by various control methods, Blum et al. (2007, 2010). In these studies, the swing leg has been modelled as a simple double pendulum. On the other hand, there have been some studies in which a linear proportional controller for a robot walking on a smooth surface has been designed when taking into account the constraint as a stopper, Ono et al. (2000, 2001, 2004); Huang et al. (2007); Sangwan et al. (2004); Mukherjee et al. (2007).

The control of swing leg, considering self-impact constraint, can be studied by two approaches. One of these approaches is that the energy which is dissipated from the system during the constraint establishment must be compensated in each gait cycle. Ono et al. (2000, 2001, 2004); Huang et al. (2007), obtained the dissipated energy due to joint self-impact stopper. In order to restore the dissipated energy per cycle, they applied a torque to the

hip joint model; this torque was determined by a simple proportional controller. This approach is appropriate for regulation purposes and not for tracking control of the (desired motion of the) swing leg during the gait cycle. Also, in these studies, joint self-impact phenomenon was considered as a constraint in the governing equations using impulse and momentum approach, which is able to model the constraint setting stage, but unable to model the constrained motion stage.

The other approach is to use an advanced controller suitable for both regulation and tracking control problems of the swing leg modeled by a movable double pendulum including the self-impact constraint. To carry out this objective, the available data of normal human gait will be considered as the desired trajectories of the hip and knee joints and the origin of the double pendulum, Ounpuu (1994); McCaw (2001).

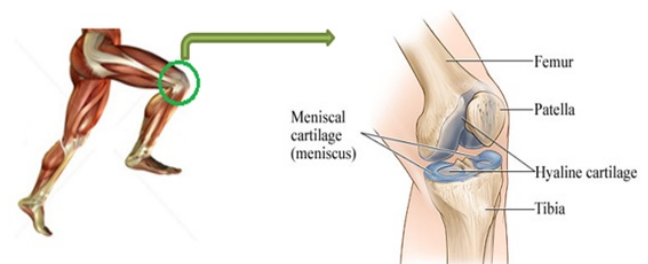


Fig. 1. Detailed schematics of knee joint

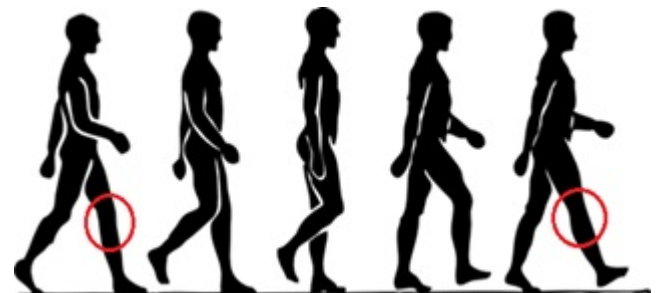


Fig. 2. Joint self-impact, when shank and thigh are aligned, in a complete period of walking

In this paper, first, modelling of a swing leg (as both fixed and movable double pendulums) considering joint self-impact constraint will be presented. Next, the control strategy for trajectory tracking control of the joint self-impact system will be presented. The proposed control method, due to the nonlinear nature of this phenomenon, is feedback linearization approach. Finally, the simulation results are reported and discussed.

## 2. MATHEMATICAL DESCRIPTION OF DYNAMICAL MODELLING

As mentioned earlier, walking is made up of two main distinct phases: SSP and DSP. According to the fact that SSP accounts for a much larger share in a walking gait cycle; this phase has been the main focus of research study in this field. In SSP, one leg appears as the swing leg and

the other one will be stationary. The swing leg is frequently modelled as a simple unconstrained double pendulum. The thigh and shank of a human leg will be represented by the links of the double pendulum whose joints, hip and knee, will connect the upper body to thigh and shank. The total moments of the leg muscles applied to move thigh and shank will be designated by two external (motor) torques applied at the hip and knee joints. The governing equations of this system will be presented in section 2.1.

The main differences in this study, compared to the previous works, are assuming the double pendulum is movable and considering the joint self-impact constraint in double pendulum modeling at the knee joint. Consequently, the mathematical modeling will be presented for two distinct cases: Case A: constrained fixed double pendulum and Case B: constrained movable double pendulum. Case A only deals with the second difference and Case B considers both differences.

In section 2.2, the joint self-impact phenomenon is modeled as a torsional spring-damper system. Then, to account for both the constraint setting and the constrained motion stages of the constraint, and to have them characterized in a unified manner, a unit step (Heaviside) function will be used for dynamical modelling of a constrained double pendulum. In order to have continuous dynamic equations, this function has to be substituted by using a suitable continuous approximation, for example an exponential function, which will be discussed in section 2.3. By using another step function approximation for the systems physical consistency, dynamics of a constrained double pendulum will be presented in section 2.4. In section 2.5, the set of the equations obtained in 2.4 will be rewritten in the state-space form which will be used in order to design a feedback linearization controller. This will complete the state-space modeling of a constrained fixed double pendulum. For the second case, the constrained movable double pendulum, to avoid lengthy presentation of the modeling, dynamic equations of the system will be derived based on Lagranges method and presented in a compact form (section 2.6) and then will be rewritten in the state space form (section 2.7).

### 2.1 Description of dynamical modelling of a swing leg as a simple unconstrained double pendulum

Fig. 3 shows schematics of an unconstrained double pendulum. In this figure,  $\theta_1$  and  $\theta_2$ , denote the hip and knee rotation angles with regard to the vertical axis, respectively.  $\tau_1$  and  $\tau_2$  are the applied external (motors) torques that move the thigh and shank links.

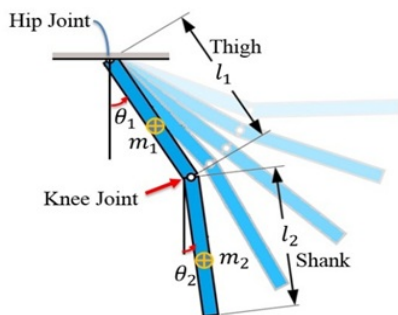


Fig. 3. Schematics of an unconstrained double pendulum

Dynamic equations of this system based on Lagranges method can be derived as follows (Singh et al. (2008)):

$$\frac{(m_1+3m_2)l_1^2\ddot{\theta}_1}{3} + \frac{m_2l_1l_2\ddot{\theta}_2 \cos(\theta_1-\theta_2)}{2} + \frac{m_2l_1l_2\dot{\theta}_2^2 \sin(\theta_1-\theta_2)}{2} + \frac{(m_1+2m_2)gl_1 \sin \theta_1}{2} = \tau_1 \quad (1)$$

$$\frac{m_2l_2^2\ddot{\theta}_2}{3} + \frac{m_2l_1l_2\dot{\theta}_1 \cos(\theta_1-\theta_2)}{2} - \frac{m_2l_1l_2\dot{\theta}_1^2 \sin(\theta_1-\theta_2)}{2} + \frac{m_2gl_2 \sin \theta_2}{2} = \tau_2 \quad (2)$$

where  $m_1, m_2$  are thigh and shank masses, and  $l_1, l_2$ , are thigh and shank lengths, respectively.

### Case A. Dynamic modeling of a swing leg as a constrained fixed double pendulum

#### 2.2 Description of dynamical modelling of joint self-impact in a constrained fixed double pendulum

For an unconstrained double pendulum,  $\theta_2$  may assume any values regardless of the amount of  $\theta_1$  rotation angle, see Fig. 3. However, for genuine mammalian legs this assumption is not valid and shank cannot assume the rotation angles which are greater than that of thigh. This discrepancy will be accounted for in system modeling by considering a self-impact constraint at the knee joint which will be activated when  $\theta_2 \geq \theta_1$ , i.e. in this situation, unlike the case for an unconstrained double pendulum, we will have  $\theta_2 = \theta_1$  for a constrained double pendulum.

Ono et al. (2000, 2001, 2004); Huang et al. (2007), considered the joint self-impact constraint as a stopper. On the other hand, Singh et al. (2008); Chatterjee et al. (1995), used a spring and damper between two colliding members to model self-impact elastic and inelastic damper. The latter is a much better choice since it models both stages of the constraint setting and the constrained motion of the joint self-impact phenomenon.

Fig. 4 shows a self-impact fixed double pendulum, Singh et al. (2008).

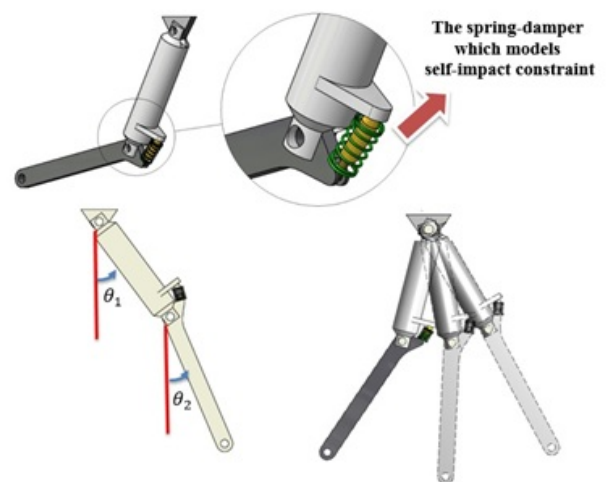


Fig. 4. Schematics of a constrained fixed double pendulum.

In Chatterjee et al. (1995) modelling, which is known as force-based method, McCaw (2001), the interaction force

is described by a linear spring-damper element. The general form of this model is:

$$F_n = c\dot{\delta} + k\delta \quad (3)$$

where,  $c$  and  $k$  are the equivalent torsional damping and stiffness coefficients, respectively.  $\delta$  and  $\dot{\delta}$  are rotation angle and angular velocity, Singh et al. (2008).

In addition, the joint self-impact phenomenon should be modeled by forces that are continually exerted between members in the time period of the activation of the constraint. Singh et al. (2008), and Chatterjee et al. (1995), used Heaviside step function in their modeling to represent this constraint for its limited activation time. Therefore, dynamical equations for joint self-impact fixed double pendulum with torsional spring and damper as joint self-impact modeling will be modified as follows:

$$\frac{(m_1+3m_2)l_1^2\ddot{\theta}_1}{3} + \frac{m_2l_1l_2\ddot{\theta}_2 \cos(\theta_1-\theta_2)}{2} + \frac{m_2l_1l_2\dot{\theta}_2^2 \sin(\theta_1-\theta_2)}{2} + \frac{(m_1+2m_2)gl_1 \sin \theta_1}{2} + U(\theta_2 - \theta_1) \left( k(\theta_1 - \theta_2) + c(\dot{\theta}_1 - \dot{\theta}_2) \right) = \tau_1 \quad (4)$$

$$\frac{m_2l_2^2\ddot{\theta}_2}{3} + \frac{m_2l_1l_2\ddot{\theta}_1 \cos(\theta_1-\theta_2)}{2} - \frac{m_2l_1l_2\dot{\theta}_1^2 \sin(\theta_1-\theta_2)}{2} + \frac{m_2gl_2 \sin \theta_2}{2} + U(\theta_2 - \theta_1) \left( k(\theta_2 - \theta_1) + c(\dot{\theta}_2 - \dot{\theta}_1) \right) = \tau_2 \quad (5)$$

### 2.3 Approximation of Heaviside step function for continuous modelling of joint self-impact constraint

In view of the fact that the step function creates discontinuities at the beginning of self-impact constraint, direct solution of equations with step function is not possible. To resolve this issue, Singh et al. (2008), and Chatterjee et al. (1995), first proposed to use the Fourier expansion (Harmonic) of the response and replaced it in the governing equations.

Since there is no harmonic forces in the joint self-impact double pendulum, Fourier expansion can cause complex nonlinear equations and substantial reduction in the accuracy of the solution. The key point is that the Heaviside step function at the joint self-impact setting stage (when  $\theta_2 = \theta_1$ ) is not differentiable. To solve the system of equations in a continuous domain, an approximation of the Heaviside function in the form of a continuous function is needed. The following is an example of a function that can be used for the approximating the Heaviside function, Singh et al. (2008):

$$U(\theta_2 - \theta_1) \approx \frac{1}{2} (1 + \tanh[r(\theta_2 - \theta_1)]) = \frac{1}{1 + e^{-2r(\theta_2 - \theta_1)}} \quad (6)$$

By increasing  $r$ , the approximation to the step function will be improved, Singh et al. (2008).

### 2.4 Physically consistent dynamical modelling of a swing leg as a constrained double pendulum

Considering the spring and damper model for joint self-impact constraint, equation (3), the joint self-impact constraint moment can be expressed as follows:

$$f_{wd}T_{ct}^1 = k(\theta_2 - \theta_1) + (\dot{\theta}_2 - \dot{\theta}_1) \quad (7)$$

$$f_{wd}T_{ct}^2 = k(\theta_1 - \theta_2) + (\dot{\theta}_1 - \dot{\theta}_2) \quad (8)$$

In general, for two rigid members undergoing self-impact constraint, the contact moments should always be positive. The condition  $f_{wd}T_{ct}^1 > 0$  is always satisfied in the above model, if the self-impact constraint at its setting stage is perfectly elastic. But since self-impact constraint is a passive phenomenon and there is some loss of energy involved at this stage, there can be a point where  $f_{wd}T_{ct}^1$  crosses 0 and becomes negative, which would imply local adhesion; however, the two members should be moving together (while the constraint is activated) or should be moving away from each other at the end of the constraint period of activation. Therefore, the constraint moment is in a direction that opposes the members separation.

To correct this physically inconsistent situation, it is necessary to ensure that the two members completely separate from each other when  $f_{wd}T_{ct}^1 = 0$ .

By replacing the above approximation in the previous equations and using approximation function for continuous improvement and correcting the physical inconsistency of the problem, the equations of motion of joint self-impact fixed double pendulum can be written as, Singh et al. (2008):

$$\frac{(m_1+3m_2)l_1^2\ddot{\theta}_1}{3} + \frac{m_2l_1l_2\ddot{\theta}_2 \cos(\theta_1-\theta_2)}{2} + \frac{m_2l_1l_2\dot{\theta}_2^2 \sin(\theta_1-\theta_2)}{2} + \frac{(m_1+2m_2)gl_1 \sin \theta_1}{2} + \frac{k(\theta_1-\theta_2)+c(\dot{\theta}_1-\dot{\theta}_2)}{(1+e^{-2r(\theta_2-\theta_1)})(1+e^{-2r(k(\theta_2-\theta_1)+c(\dot{\theta}_2-\dot{\theta}_1))})} = \tau_1 \quad (9)$$

$$\frac{m_2l_2^2\ddot{\theta}_2}{3} + \frac{m_2l_1l_2\ddot{\theta}_1 \cos(\theta_1-\theta_2)}{2} - \frac{m_2l_1l_2\dot{\theta}_1^2 \sin(\theta_1-\theta_2)}{2} + \frac{m_2gl_2 \sin \theta_2}{2} + \frac{k(\theta_2-\theta_1)+c(\dot{\theta}_2-\dot{\theta}_1)}{(1+e^{-2r(\theta_2-\theta_1)})(1+e^{-2r(k(\theta_2-\theta_1)+c(\dot{\theta}_2-\dot{\theta}_1))})} = \tau_2 \quad (10)$$

The above dynamical equations can be rewritten in a compact form as follows:

$$M_A(q)\ddot{q} + C_A(q, \dot{q})\dot{q} + G_A(q) + \tau_{fA}(q, \dot{q}) = \tau_A \quad (11)$$

where,

$$q_A = [\theta_1, \theta_2]^T, M_A = \begin{bmatrix} m_{A11} & m_{A12} \\ m_{A21} & m_{A22} \end{bmatrix}, \tau_A = \begin{bmatrix} \tau_{A1} \\ \tau_{A2} \end{bmatrix}$$

$$C_A = \begin{bmatrix} c_{A11} & c_{A12} \\ c_{A21} & c_{A22} \end{bmatrix}, G_A = \begin{bmatrix} g_{A1} \\ g_{A2} \end{bmatrix}, \tau_{fA} = \begin{bmatrix} \tau_{fA1} \\ \tau_{fA2} \end{bmatrix}$$

where the components  $m_{Aij}$ ,  $c_{Aij}$ ,  $g_{Ai}$  and  $\tau_{fAi}$  will be presented in Appendix A.

### 2.5 State space representation of a swing leg as a constrained fixed double pendulum

The set of dynamical equations of a swing leg modelled as a constrained fixed double pendulum, equation (11), may be represented as follows:

$$\ddot{q} = \nu_A = M_A^{-1} \{ \tau_A - (C_A(q, \dot{q})\dot{q} + G_A(q) + \tau_{fA}(q, \dot{q})) \} \quad (12)$$

where  $\nu_A$  is a  $2 \times 1$  vector. By defining the state variables,  $\{x_{A1} = \theta_1 = q_1, x_{A2} = \dot{\theta}_1 = \dot{q}_1, x_{A3} = \theta_2 = q_2, x_{A4} = \dot{\theta}_2 = \dot{q}_2\}$ , the state-space form of the dynamical equations may be

developed as follows:

$$\begin{aligned}\dot{x}_{A_1} &= x_{A_2} \\ \dot{x}_{A_2} &= \nu_{A_1} \\ \dot{x}_{A_3} &= x_{A_4} \\ \dot{x}_{A_4} &= \nu_{A_2}\end{aligned}\quad (13)$$

Also, the output variables are:

$$y_{A_1} = x_{A_1} \quad (14)$$

$$y_{A_2} = x_{A_3} \quad (15)$$

and the input control variables are:

$$u_{A_1} = \tau_{A_1} \quad (16)$$

$$u_{A_2} = \tau_{A_2} \quad (17)$$

The above model of a swing leg as a constrained fixed double pendulum can be written, for further study, in a compact affine form as:

$$\dot{x} = f(x) + g(x)u \quad (18)$$

$$y = h(x) \quad (19)$$

## Case B. Dynamic modeling of a swing leg as a constrained movable double pendulum

### 2.6 Dynamic modeling of a swing leg as a constrained movable double pendulum

Fig. 5 shows schematics of a constrained movable double pendulum.

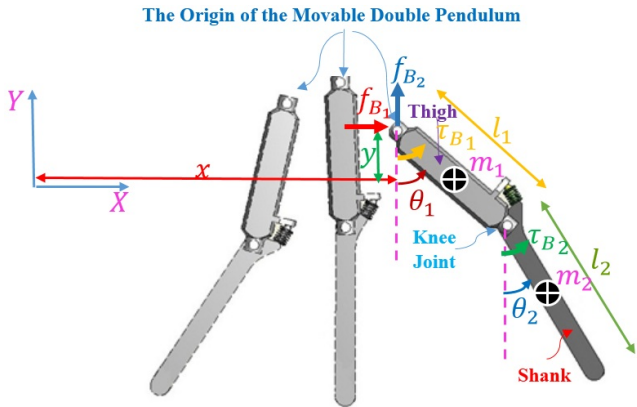


Fig. 5. Schematics of a constrained movable double pendulum

In this figure,  $\theta_1$  and  $\theta_2$ , denote the hip and knee rotation angles with regard to the vertical axis, respectively and  $x$  and  $y$  denote the horizontal and vertical displacements of the origin of the double pendulum, respectively. Also,  $\tau_{B_1}$  and  $\tau_{B_2}$  are the applied external (motors) torques that move the thigh and shank links, also  $f_{B_1}$  and  $f_{B_2}$  are the applied external forces that move the origin of the double pendulum. Dynamic equations of this system based on Lagranges method can be derived in a compact form as follows:

$$M_B(q)\ddot{q} + C_B(q, \dot{q})\dot{q} + G_B(q) + \tau_{fB}(q, \dot{q}) = \tau_B \quad (20)$$

where,

$$q_B = [x, y, \theta_1, \theta_2]^T, M_B = \begin{bmatrix} m_{B_{11}} & m_{B_{12}} & m_{B_{13}} & m_{B_{14}} \\ m_{B_{21}} & m_{B_{22}} & m_{B_{23}} & m_{B_{24}} \\ m_{B_{31}} & m_{B_{32}} & m_{B_{33}} & m_{B_{34}} \\ m_{B_{41}} & m_{B_{42}} & m_{B_{43}} & m_{B_{44}} \end{bmatrix},$$

$$C_B = \begin{bmatrix} c_{B_{11}} & c_{B_{12}} & c_{B_{13}} & c_{B_{14}} \\ c_{B_{21}} & c_{B_{22}} & c_{B_{23}} & c_{B_{24}} \\ c_{B_{31}} & c_{B_{32}} & c_{B_{33}} & c_{B_{34}} \\ c_{B_{41}} & c_{B_{42}} & c_{B_{43}} & c_{B_{44}} \end{bmatrix}, G_B = \begin{bmatrix} g_{B_1} \\ g_{B_2} \\ g_{B_3} \\ g_{B_4} \end{bmatrix}, \tau_B = \begin{bmatrix} f_{B_1} \\ f_{B_2} \\ \tau_{B_1} \\ \tau_{B_2} \end{bmatrix},$$

$$\tau_{fB}(\theta, \dot{\theta}) = \begin{bmatrix} 0 \\ 0 \\ \frac{(k(\theta_1 - \theta_2) + c(\dot{\theta}_1 - \dot{\theta}_2))}{(1 + e^{-2r(\theta_2 - \theta_1)})(1 + e^{-2r(k(\theta_2 - \theta_1) + c(\dot{\theta}_2 - \dot{\theta}_1)))}} \\ \frac{(k(\theta_2 - \theta_1) + c(\dot{\theta}_2 - \dot{\theta}_1))}{(1 + e^{-2r(\theta_2 - \theta_1)})(1 + e^{-2r(k(\theta_2 - \theta_1) + c(\dot{\theta}_2 - \dot{\theta}_1)))}} \end{bmatrix},$$

where the components  $m_{B_{ij}}$ ,  $c_{B_{ij}}$  and  $g_{B_i}$  will be presented in Appendix B.

### 2.7 State space representation of a swing leg as a constrained movable double pendulum

The set of dynamical equations of a swing leg modelled as a constrained movable double pendulum, equation (20), may be represented as follows:

$$\ddot{q}_B = \nu_B = M_B^{-1} \{ \tau_B - (C_B(q, \dot{q})\dot{q} + G_B(q) + \tau_{fB}(q, \dot{q})) \} \quad (21)$$

where  $\nu_B$  is a  $4 \times 1$  vector. By defining the state variables,

$$\begin{cases} x_{B_1} = x = q_1, x_{B_2} = \dot{x} = \dot{q}_1, x_{B_3} = y = q_2, \\ x_{B_4} = \dot{y} = \dot{q}_2, x_{B_5} = \theta_1 = q_3, x_{B_6} = \dot{\theta}_1 = \dot{q}_3, \\ x_{B_7} = \theta_2 = q_4, x_{B_8} = \dot{\theta}_2 = \dot{q}_4 \end{cases}$$

the state-space form of the dynamical equations may be developed as follows:

$$\begin{aligned}\dot{x}_{B_1} &= x_{B_2} \\ \dot{x}_{B_2} &= \nu_{B_1} \\ \dot{x}_{B_3} &= x_{B_4} \\ \dot{x}_{B_4} &= \nu_{B_2} \\ \dot{x}_{B_5} &= x_{B_6} \\ \dot{x}_{B_6} &= \nu_{B_3} \\ \dot{x}_{B_7} &= x_{B_8} \\ \dot{x}_{B_8} &= \nu_{B_4}\end{aligned}\quad (22)$$

Also, the output variables are:

$$y_{B_1} = x_{B_1} \quad (23)$$

$$y_{B_2} = x_{B_3} \quad (24)$$

$$y_{B_3} = x_{B_5} \quad (25)$$

$$y_{B_4} = x_{B_7} \quad (26)$$

and the input control variables are:

$$u_{B_1} = f_{B_1} \quad (27)$$

$$u_{B_2} = f_{B_2} \quad (28)$$

$$u_{B_3} = \tau_{B_1} \quad (29)$$

$$u_{B_4} = \tau_{B_2} \quad (30)$$

The above model of a swing leg as a constrained movable double pendulum can also be written in the compact affine form of equations (18), (19).

### 3. TRACKING CONTROL OF THE JOINT SELF-IMPACT SYSTEM

To the best our knowledge, there has not been any publication on tracking control of any joint self-impact system. However, there are a few articles on regulation problem of the constrained double pendulum system by some researchers, Ono et al. (2000, 2001, 2004); Huang et al. (2007); Sangwan et al. (2004); Mukherjee et al. (2007), and also by the authors, Bazargan-Lari et al. (2011).

For the tracking problem, the gait cycles of normal walking taken from the available data, Ounpuu (1994); McCaw (2001), should be assigned as the desired trajectories of the thigh and knee joints of the constrained double pendulum. Due to complex nonlinear terms in the system dynamics equations of self-impact double pendulum, we propose to design a nonlinear model-based controller by taking advantage of the feedback linearization control method, which is a well-known fundamental and prevailing method for complex nonlinear systems.

#### 3.1 Feedback linearization

By input-output linearization it is meant the generation of a linear differential relation between the output  $y$  and a new input  $\nu$ , Slotine et al. (1991). The general system dynamical equations can be written in the affine form equations (18), (19).

Given the nonlinear system in equation (18) and equation (19), input-output linearization of the system is obtained by first differentiating the output  $y_i$  until all inputs appear. Assume that  $r_i$  is the smallest integer such that at least one of the inputs appears in  $y_i^{r_i}$ , then,

$$y_i^{r_i} = L_f^{r_i} h_i + \sum_{j=1}^m L_{g_j} L_f^{r_i-1} h_i u_j \quad (31)$$

with  $L_{g_j} L_f^{r_i-1} h_i(x) \neq 0$  for at least one output. Performing the above procedure for each output  $y_i$ , yields:

$$\begin{bmatrix} y_1^{r_1} \\ \vdots \\ y_m^{r_m} \end{bmatrix} = \begin{bmatrix} L_f^{r_1} h_1 \\ \vdots \\ L_f^{r_m} h_m \end{bmatrix} + E(x)u \quad (32)$$

where,  $L_f h = \nabla h \cdot f$ ,  $h : R^n \rightarrow R$  is a smooth scalar function,  $f : R^n \rightarrow R^n$  is a smooth vector field on  $R^n$  and the  $m \times m$  matrix  $E(x)$  is systematically obtained during taking the derivatives of the outputs. If, as assumed above, the partial relative degrees (relative degree of a nonlinear system is equal to required number of differentiation of the output of a system to generate an explicit relationship between the output  $y$  and input  $u$ )  $r_i$  are all well defined, then  $\Omega$  is a finite neighborhood of  $x_0$ . Furthermore, if  $E(x)$  is invertible over the region  $\Omega$ , then, input transformation is:

$$u = E^{-1} \begin{bmatrix} \nu_1 - L_f^{r_1} h_1 \\ \vdots \\ \nu_m - L_f^{r_m} h_m \end{bmatrix} \quad (33)$$

which yields  $m$  equations of the simple form

$$y_i^{r_i} = \nu_i \quad (34)$$

Since the input  $\nu_i$  only affects the output  $y_i$  as in equation (34), it is called a decoupling control law, and the invertible

matrix  $E(x)$  is called the decoupling matrix of the system, Slotine et al. (1991). The system of equations (18) and (19) is then said to have relative degrees  $(r_1, r_2, \dots, r_m)$  at  $x_0$ , and the scalar  $r = (r_1 + r_2 + \dots + r_m)$  is called the total relative degree of the system at  $x_0$ .

#### 3.2 Controller design

To apply the input-output feedback linearization procedure, the outputs are differentiated until the inputs are all appeared in the equations. For both cases A and B, we have to take the second derivatives to see all the inputs.

**Case A:**

$$\ddot{y}_{A_i} = \nu_{A_i} = \sum_{j=1}^2 h_{ij} \tau_j - \sum_{j=1}^2 h_{ij} (C_A \dot{q} + G_A + \tau_{fA})_j \quad (35)$$

$$i = 1, 2$$

where,  $h_{A_{ij}} = (M_A^{-1})_{ij}$  and  $(C_A \dot{q} + G_A + \tau_{fA})_j$  shows the  $j^{th}$  component of the vector  $(C_A \dot{q} + G_A + \tau_{fA})$ .

**Case B:**

$$\ddot{y}_{B_i} = \nu_{B_i} = \sum_{j=1}^4 h_{ij} \tau_j - \sum_{j=1}^4 h_{ij} (C_B \dot{q} + G_B + \tau_{fB})_j \quad (36)$$

$$i = 1, 2, 3, 4$$

where,  $h_{B_{ij}} = (M_B^{-1})_{ij}$  and  $(C_B \dot{q} + G_B + \tau_{fB})_j$  shows the  $j^{th}$  component of the vector  $(C_B \dot{q} + G_B + \tau_{fB})$ .

Comparing equation (32) with equations (12) and (21) reveals that  $E_A(x) = M_A^{-1}$ ,  $E_B(x) = M_B^{-1}$ . Since  $M_A^{-1}$  and  $M_B^{-1}$  are positive definite,  $E_A$  and  $E_B$  will be non-singular and therefore, they are invertible. As it can be seen from the above equations, the total relative degree of the both systems, is equal to 4 for case A and 8 for case B, respectively. Therefore, both of them have no internal dynamics, Slotine et al. (1991). Then, the control inputs can be calculated from equation (33) as follows:

**Case A:**

$$u_{A_i} = \sum_{j=1}^2 m_{A_{ij}} \nu_{A_j} - h_{A_{ij}} (C_A \dot{q} + G_A)_j \quad (37)$$

$$i = 1, 2$$

**Case B:**

$$u_{B_i} = \sum_{j=1}^4 m_{B_{ij}} \nu_{B_j} - h_{B_{ij}} (C_B \dot{q} + G_B)_j \quad (38)$$

$$i = 1, 2, 3, 4$$

The above inputs transform the output equations to the simple form of equation (34), and; therefore, the external dynamics can be easily controlled by any linear technique. The controller can be tuned, by applying four coefficients,  $k_{A_{P_1}}, k_{A_{P_2}}, k_{A_{D_1}}, k_{A_{D_1}}$ , for case A and eight coefficients,  $k_{B_{P_1}}, k_{B_{P_2}}, k_{B_{P_3}}, k_{B_{P_4}}, k_{B_{D_1}}, k_{B_{D_2}}, k_{B_{D_3}}, k_{B_{D_4}}$  for case B, as the controller gains, in order to track the desired trajectories. The decoupling control laws may be defined as follows:

**Case A:**

$$\nu_{A_i} = \ddot{y}_{id} - k_{A_{P_i}} e_i - k_{A_{D_i}} \nu_{A_i} \quad i = 1, 2 \quad (39)$$

where,  $e_{A_i} = \theta_{A_i} - \theta_{A_{id}}$ ,  $\dot{e}_{A_i} = \dot{\theta}_{A_i} - \dot{\theta}_{A_{id}}$

**Case B:**

$$\nu_{B_i} = \ddot{y}_{id} - k_{B_{P_i}} e_i - k_{B_{D_i}} \nu_{B_i} \quad i = 1, 2, 3, 4 \quad (40)$$

where,  $e_{Bi} = \theta_{Bi} - \theta_{Bid}$ ,  $\dot{e}_{Bi} = \dot{\theta}_{Bi} - \dot{\theta}_{Bid}$   
 Applying the decoupling control law in the exactly linearized equations of, equation (34), leads to the following tracking error dynamics:

**Case A:**  

$$\ddot{e}_{Ai} = k_{ADi}\dot{e}_{Ai} + k_{APi}e_{Ai} = 0 \quad i = 1, 2 \quad (41)$$

**Case B:**  

$$\ddot{e}_{Bi} = k_{BDi}\dot{e}_{Bi} + k_{BPi}e_{Bi} = 0 \quad i = 1, 2, 3, 4 \quad (42)$$

By choosing positive values for the constants  $k_{APi}, k_{ADi}, k_{BPi}$  and  $k_{BDi}$ , both of the above error dynamics are exponentially stable.

4. SIMULATIONS AND DISCUSSION

Table 1 shows the parameters that are used to simulate the locomotion of a swing leg as a self-impact double pendulum. The anthropometric dimensions and masses match the parameters presented in reference, McCaw (2001).

Table 1. The parameters used to simulate the leg locomotion as a self-impact double pendulum

Parameter	Description	Value
$m_1, m_2$	Masses of thigh and shank links	0.1 kg
$l_1, l_2$	Lengths of thigh and shank links	0.55 m
$c$	Damping coefficient	2.4 N · s/rad
$k$	Stiffness coefficient	42 N/rad
$r$	Accuracy of the approximating function	10e5

4.1 The gait cycles of normal walking taken as the desired joint angles of the hip and knee joints and the desired horizontal and vertical displacements of the origin of the double pendulum

For the tracking problem, the desired trajectories of the thigh and knee joints and the origin of the double pendulum, representing the swing leg during normal walking, should be taken from the available normal gait cycle data, Ounpuu (1994); McCaw (2001).

The desired trajectories are presented in Figs. 6, 7, 8; the period in which the joint self-impact phenomenon occurs is highlighted in Fig. 6.

According to Fig. 6, joint self-impact phenomenon for joint self-impact double pendulum system happens when the knee rotation angle is greater than that of the hip.

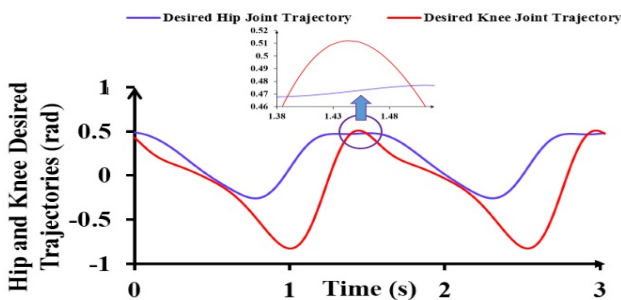


Fig. 6. Human's hip and knee normal gait cycles, (Ounpuu (1994))

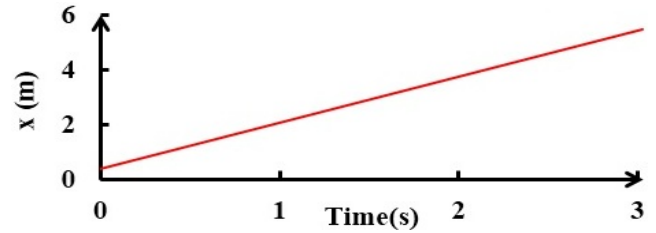


Fig. 7. Desired horizontal displacement of the origin of the constrained movable double pendulum.

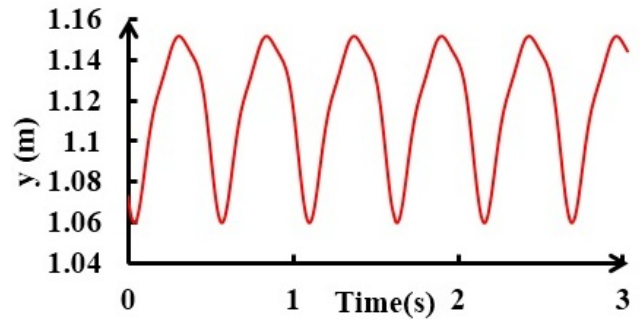


Fig. 8. Desired vertical displacement of the origin of the constrained movable double pendulum.

Taking the time derivative of these curves, the desired angular velocities of the hip and knee joints and the desired horizontal and vertical velocities of the origin of the double pendulum will be obtained, see Figs 9, 10.

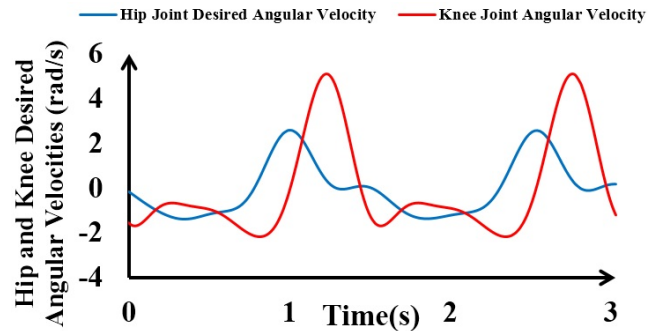


Fig. 9. Human's hip and knee desired angular velocities

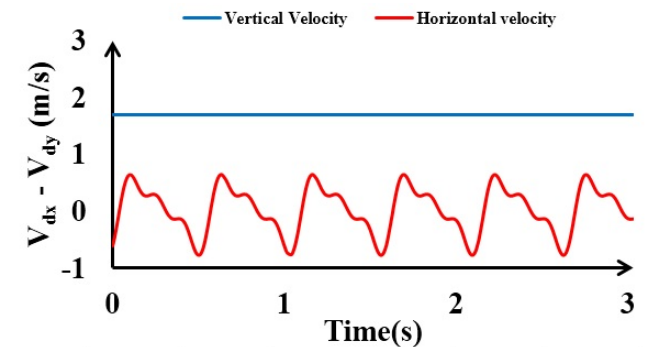


Fig. 10. Desired horizontal and vertical velocities of the origin of the constrained movable double pendulum as a swing leg in normal walking

4.2 The block diagram of the proposed controller

In this article, feedback linearization method is proposed to be used for the trajectory tracking of a constrained double pendulum. The block diagram of the proposed controller is illustrated in Fig. 11.

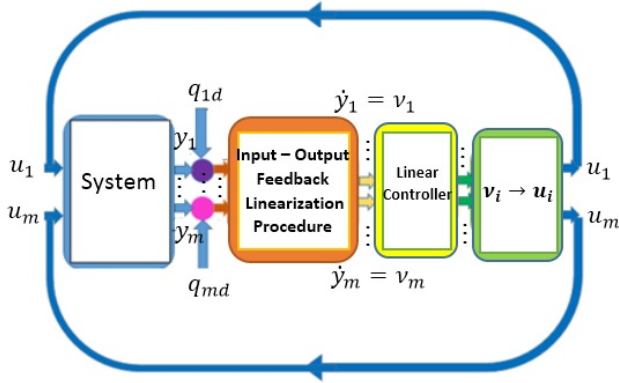


Fig. 11. Controller block diagram

4.3 Self-impact double pendulum simulation results

Case A. Simulation results for a swing leg as a constrained fixed double pendulum

The purpose of this case is to simulate the tracking control of the self-impact fixed double pendulum. Fig. 12 shows the hip joint desired and tracked trajectories, which is well followed by the swing leg. Time history of hip joint angle error is shown in Fig. 13. As already seen in Fig. 6, the joint self-impact constraint is activated in the time period of 1.38 to 1.52 sec. In this period, the swing leg hip joint follows the desired trajectory with an acceptable maximum error of about 0.007%. The same results are established for knee joint in Figs. 14 and 15 and the maximum error is about 0.013%. As seen in Figs. 12, 13, 14, 15, the performance of the controller is acceptable. As it can be seen in the figures, when the constraint is activated, the hip and knee joint angular velocity and the applied torque of the motor suddenly changes in both joints. Despite this sudden changes, the controller follows the trajectories of thigh and knee joints accurately.

Fig. 16 shows the time history of the tracked angular velocity of the hip joint together with its desired angular velocity. As seen in the figure, in the time period of 1.38 to 1.52 sec, the swing leg is encountered with a sudden change in its speed, which is caused by an increase in the angular momentum of the link due to the establishment of the constraint. The controller has matched the hip joint speed to its desired value with the maximum error of about 0.15%. For knee joint velocity, the maximum error is about 0.035%. Figs. 18 and 19 represent the amount of torques applied by the motors embedded in the hip and knee joints, respectively. When joint self-impact constraint is activated, the moment caused by the establishment of the constraint is in the same direction of the motor torque of the hip joint, which causes the motor to provide less torque to track the path. These figures show the sudden drop in the amount of torques.

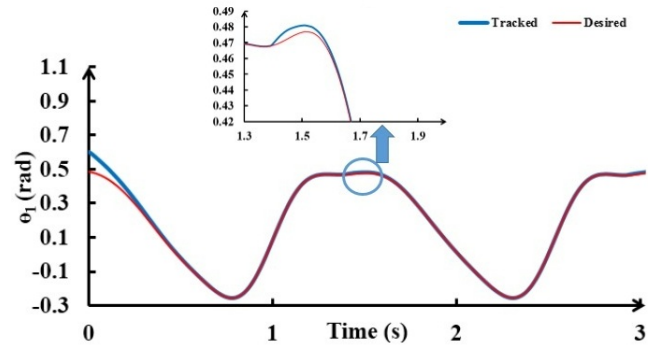


Fig. 12. Hip joint desired and tracked trajectories

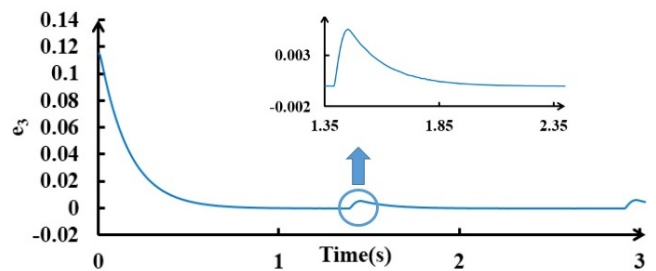


Fig. 13. Time history of error of the hip joint angle.

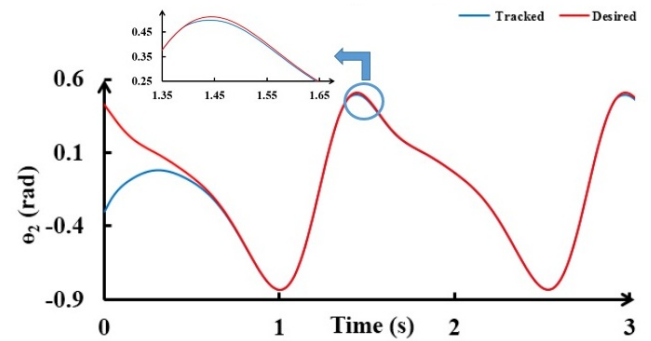


Fig. 14. Knee joint desired and tracked trajectories.

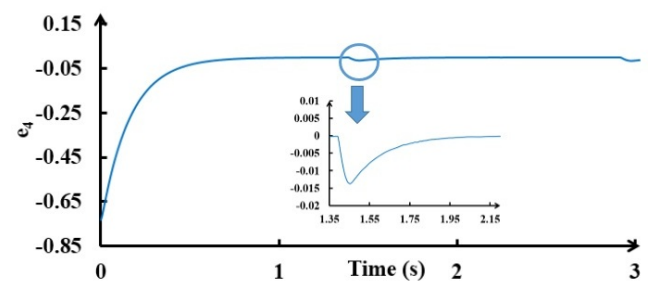


Fig. 15. Time history of error of the knee joint angle.

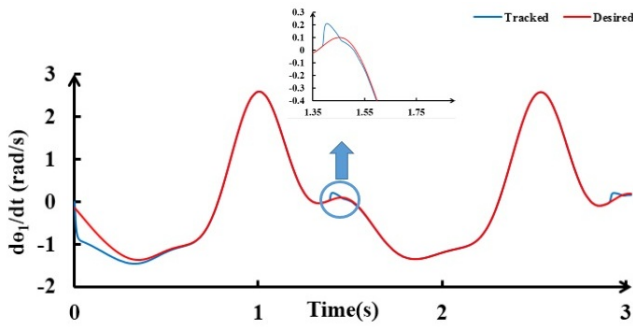


Fig. 16. Time history of the hip joint desired and tracked angular velocities.

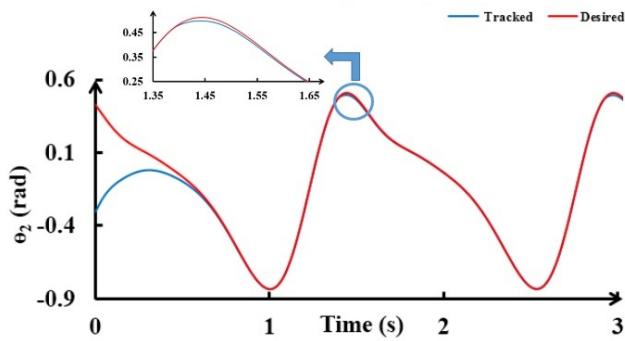


Fig. 17. Time history of the knee joint desired and tracked angular velocities.

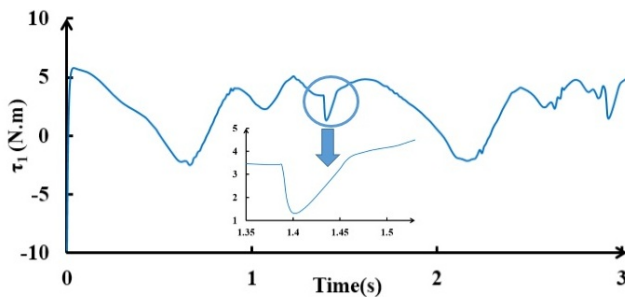


Fig. 18. Time history of the hip joint applied torque.

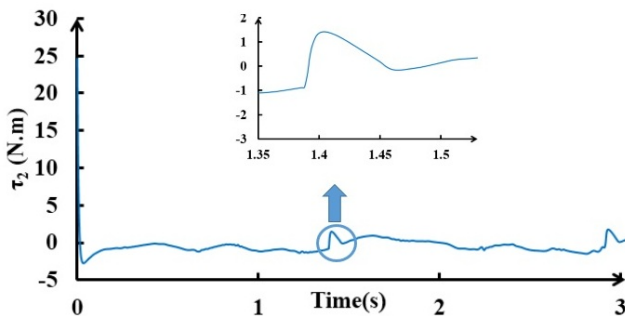


Fig. 19. Time history of the knee joint applied torque.

**Case B. Simulation results for a swing leg as a constrained movable double pendulum**

The purpose of the this case is to simulate the tracking control of the self-impact movable double pendulum. Figs. 20

and 21 show desired horizontal and vertical displacement of the origin of the constrained movable double pendulum and tracked trajectories, which are well followed by the swing leg. moreover, Fig. 22 shows the hip joint desired and tracked trajectories, which is well followed by the swing leg. Time history of hip joint angle error is shown in Fig. 23. In the period of activation of the constraint, Fig. 6, the swing leg hip joint follows the desired trajectory with an acceptable maximum error of about 0.005%. The same results are established for the knee joint in Figs 25 and 24 and the maximum error is about 0.0072%. As seen in Figs. 20, 21,22, 23, 25, 24 the performance of controller is acceptable. As it can be seen in the figures, when the constraint is activated, horizontal and vertical velocity of the origin of the constrained movable pendulum and the hip and knee joint angular velocity and the applied torque of the motor suddenly changes in both joints. Despite this sudden changes, the controller follows the Desired trajectories accurately.

Figs. 26, 27 show the horizontal and vertical velocities of the origin of the constrained movable double pendulum with their desired velocities, respectively. Also, Figs. 28, 29 illustrate the time history of the desired and tracked angular velocities of the hip and knee joints, respectively. As seen in the figures, in the time period of 1.38 to 1.52 sec, the swing leg is encountered with a sudden change in its speed, which is caused by an increase in the angular momentum of the link due to the establishment of the constraint. The controller has matched the joint's speed to their desired values with the maximum error of about 0.25%.

Figs. 30, 31, 32, 33 represent the amount of forces and torques applied by the motors embedded in the hip and knee joints, respectively. When joint self-impact constraint is activated, the moment caused by the establishment of the constraint is in the same direction of the motor torques of the joints, which cause the motor to provide less torque to track the path. These figures show the sudden drop in the amount of torques.

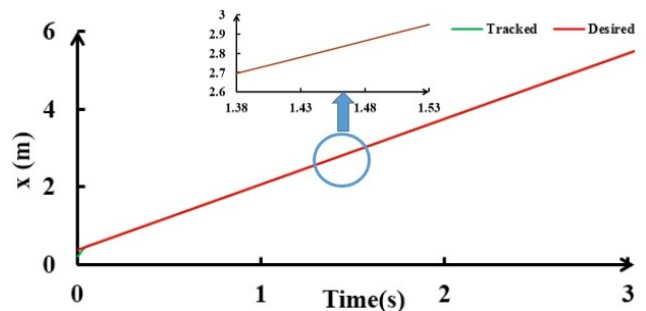


Fig. 20. Horizontal displacement of the origin of the constrained movable double pendulum desired-tracked trajectories.

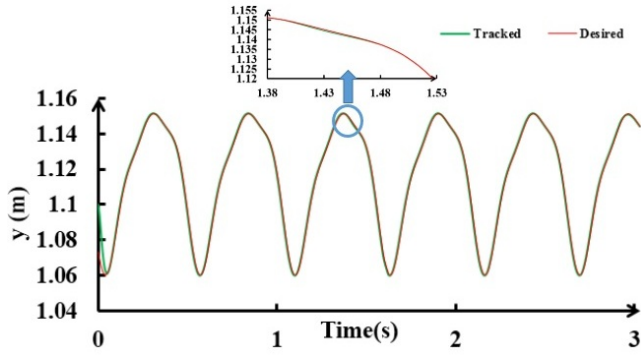


Fig. 21. Vertical displacement of the origin of the constrained movable double pendulum desired-tracked trajectories.

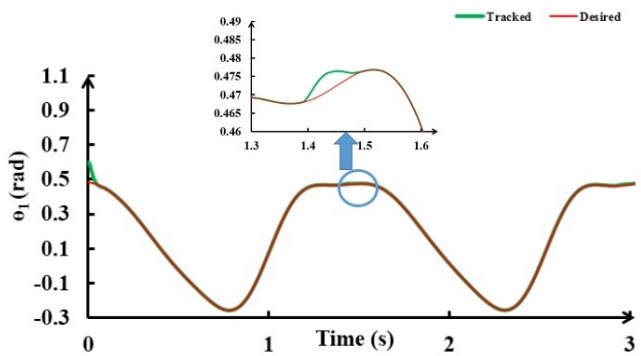


Fig. 22. Hip joint desired and tracked trajectories.

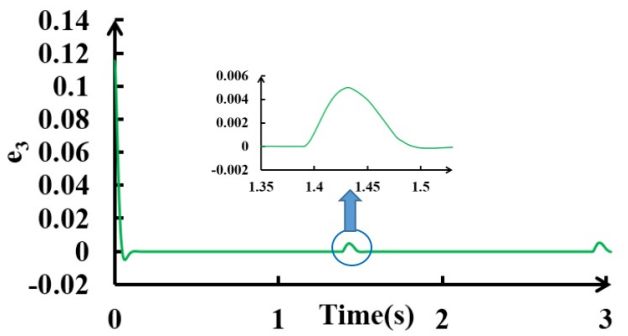


Fig. 23. Time history of error of the hip joint angle.

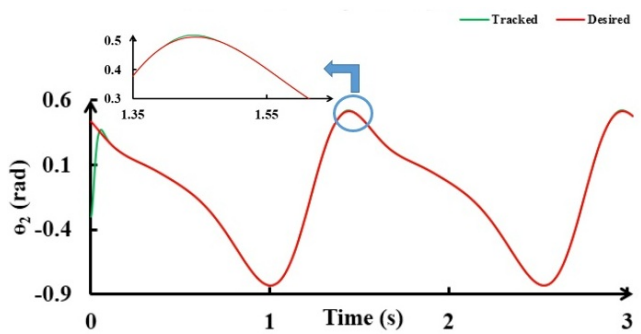


Fig. 24. Knee joint desired and tracked trajectories.

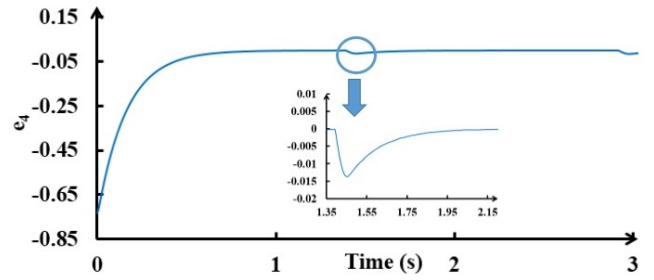


Fig. 25. Time history of error of the knee joint angle.

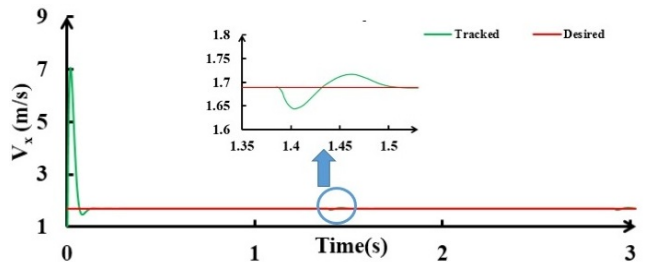


Fig. 26. Desired and tracked horizontal velocity of the origin of the constrained movable double pendulum.

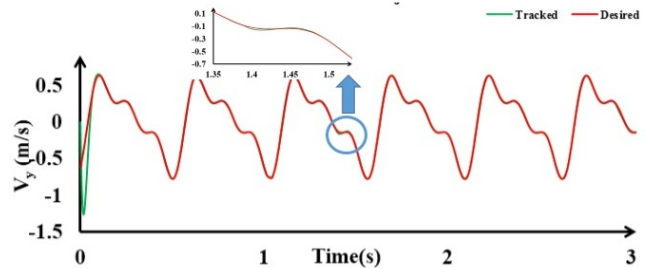


Fig. 27. Desired and tracked vertical velocity of the origin of the constrained movable double pendulum.

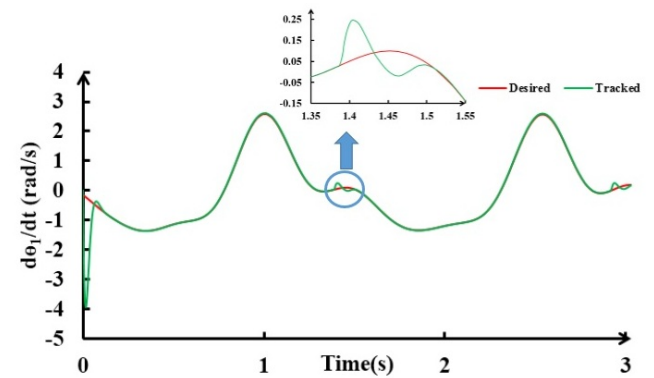


Fig. 28. Time history of the hip joint desired and tracked angular velocities (Movable).

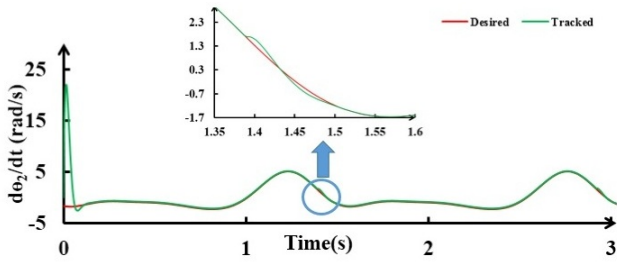


Fig. 29. Time history of the knee joint desired and tracked angular velocities (Movable).

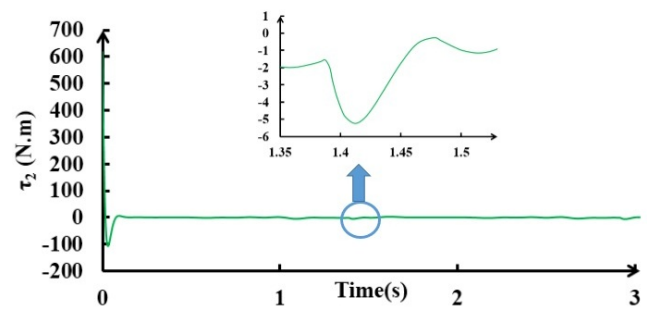


Fig. 33. Time history of the applied Knee joint torque(movable).

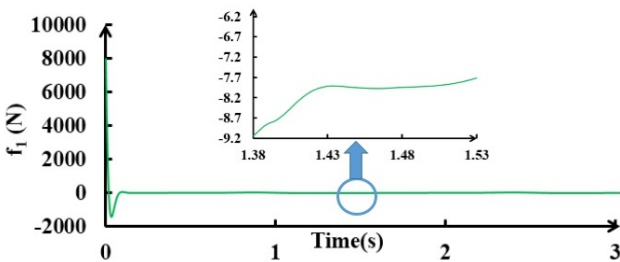


Fig. 30. Time history of the applied horizontal force at the origin of the constrained movable double pendulum.

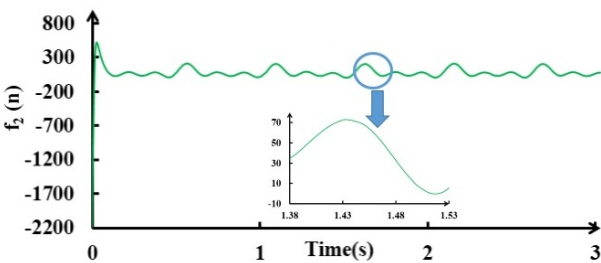


Fig. 31. Time history of the applied vertical force at the origin of the constrained movable double pendulum.

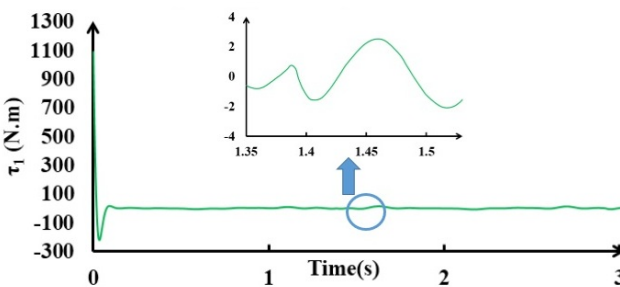


Fig. 32. Time history of the applied Hip joint torque (movable).

## 5. CONCLUSION

The objectives of this paper were to present a model-based control method for trajectory tracking of both joint self-impact constrained fixed and movable double pendulums which model the swing leg in normal human walking. To achieve the objectives, first, the dynamical equations of motion of an unconstrained double pendulum were taken and then developed and modified to account for the joint self-impact constraint at the knee joint and also movable origin of the double pendulum. Two approximations of the Heaviside step function were applied to the equations of motion in order to account for continuity and physical consistency of the derived set of equations of motion. To control these complicated systems, the available normal gait cycle data were taken to generate the desired trajectories of the thigh and knee joints and the horizontal and vertical displacements of the origin of the double pendulum. The control method used in this paper, due to the nonlinear nature of the joint self-impact constrained fixed and movable double pendulums, was feedback linearization approach.

According to the simulation results, the normal gait cycle data of the rotation angles of the hip and knee joints and the horizontal and vertical displacements of the origin of the double pendulum were well followed by the simulated constrained double pendulums. The joint self-impact constraint was activated in the time period of 1.38 to 1.52 sec. In this period, even in the presence of the sudden changes in the hip and knee kinematic variables at the constraint activation stage, the swing leg (double pendulum) kinematic variables tracked their desired values with acceptable maximum errors.

## REFERENCES

- Ayyappa, E. (1997). Normal human locomotion, part 1: Basic concepts and terminology. *JPO: Journal of Prosthetics and Orthotics*, 9(1), 10–17.
- Bazargan-Lari, Y., Gholipour, A., Eghtesad, M., Nouri, M., and Sayadkooh, A. (2011). Dynamics and control of locomotion of one leg walking as self-impact double pendulum. In *Control, Instrumentation and Automation (ICCIA), 2011 2nd International Conference on*, 201–206. IEEE.
- Blum, Y., Lipfert, S., Rummel, J., and Seyfarth, A. (2010). Swing leg control in human running. *Bioinspiration & biomimetics*, 5(2), 026006.

- Blum, Y., Rummel, J., and Seyfarth, A. (2007). Advanced swing leg control for stable locomotion. In *Autonome Mobile Systeme 2007*, 301–307. Springer.
- Chatterjee, S., Mallik, A., and Ghosh, A. (1995). On impact dampers for non-linear vibrating systems. *Journal of Sound and Vibration*, 187(3), 403–420.
- Couceiro, M.S., Ferreira, N., and Machado, J. (2010). Modeling and control of a dragonfly-like robot. *Journal of Control Science and Engineering*, 2010, 5.
- Couceiro, M.S., Ferreira, N.F., and Machado, J.T. (2009). Fractional-order control of a robotic bird. In *ASME 2009 International Design Engineering Technical Conferences and Computers and Information in Engineering Conference*, 163–169. American Society of Mechanical Engineers.
- Couceiro, M.S., Ferreira, N.M., and Machado, J. (2012). Hybrid adaptive control of a dragonfly model. *Communications in Nonlinear Science and Numerical Simulation*, 17(2), 893–903.
- Couceiro, M.S., Figueiredo, C.M., Ferreira, N.F., and Machado, J.T. (2008). Simulation of a robotic bird. *Fractional differentiation and its applications, Ankara*.
- Cross, R. (2011). A double pendulum model of tennis strokes. *American Journal of Physics*, 79(5), 470–476.
- Goswami, A., Espiau, B., and Keramane, A. (1997). Limit cycles in a passive compass gait biped and passivity-mimicking control laws. *Autonomous Robots*, 4(3), 273–286.
- Huang, Q., Hase, T., and Ono, K. (2007). Passive/active unified dynamic walking for biped locomotion. In *Robotics and Biomimetics, 2007. ROBIO 2007. IEEE International Conference on*, 964–971. IEEE.
- McCaw, S.T. (2001). Introduction to biomechanics. *Foundations of Exercise Science*, 155.
- Miller, R.H. (2011). Optimal control of human running.
- Mukherjee, S., wan, V., Taneja, A., and Seth, B. (2007). Stability of an underactuated bipedal gait. *Biosystems*, 90(2), 582–589.
- Ono, K., Furuichi, T., and Takahashi, R. (2004). Self-excited walking of a biped mechanism with feet. *The International Journal of Robotics Research*, 23(1), 55–68.
- Ono, K., Takahashi, R., Imadu, A., and Shimada, T. (2000). Self-excitation control for biped walking mechanism. In *Intelligent Robots and Systems, 2000. (IROS 2000). Proceedings. 2000 IEEE/RSJ International Conference on*, volume 2, 1143–1148. IEEE.
- Ono, K., Takahashi, R., and Shimada, T. (2001). Self-excited walking of a biped mechanism. *The International Journal of Robotics Research*, 20(12), 953–966.
- Ounpuu, S. (1994). The biomechanics of walking and running. *Clinics in sports medicine*, 13(4), 843–863.
- Rose, J., Gamble, J.G., and Adams, J.M. (2006). *Human walking*. Lippincott Williams & Wilkins Philadelphia.
- Sangwan, V., Taneja, A., and Mukherjee, S. (2004). Design of a robust self-excited biped walking mechanism. *Mechanism and machine theory*, 39(12), 1385–1397.
- Singh, S., Mukherjee, S., and Sanghi, S. (2008). Study of a self-impacting double pendulum. *Journal of sound and vibration*, 318(4), 1180–1196.
- Slotine, J.J.E., Li, W., et al. (1991). *Applied nonlinear control*, volume 199. Prentice-Hall Englewood Cliffs, NJ.
- Zhang, D. and Zhu, K. (2006). Model and control of the locomotion of a biomimic musculoskeletal biped. *Artificial Life and Robotics*, 10(2), 91–95.

Appendix A. CASE A, COMPONENTS OF THE MATRICES  $M_A$  AND  $C_A$  AND THE VECTORS  $G_A$  AND  $\tau_{FA}$

$$\begin{aligned}
 m_{A11} &= \frac{m_1+3m_2}{3}l_1^2, m_{A12} = \frac{m_2l_1l_2}{2} \cos(\theta_1 - \theta_2) \\
 m_{A21} &= \frac{m_2l_1l_2}{2} \cos(\theta_1 - \theta_2), m_{A22} = \frac{m_2}{3}l_2^2 \\
 c_{A11} &= 0, c_{A12} = \frac{m_2l_1l_2}{2} \sin(\theta_1 - \theta_2)\dot{\theta}_2 \\
 c_{A21} &= -\frac{m_2l_1l_2}{2} \sin(\theta_1 - \theta_2)\dot{\theta}_1, c_{A22} = 0 \\
 g_{A1} &= \frac{m_1 + 2m_2}{2}gl_1 \sin \theta_1, g_{A2} = \frac{m_2}{2}gl_2 \sin \theta_2 \\
 \tau_{fA1} &= \frac{\left(k(\theta_1 - \theta_2) + c(\dot{\theta}_1 - \dot{\theta}_2)\right)}{\left(1 + e^{-2r(\theta_2 - \theta_1)}\right) \left(1 + e^{-2r(k(\theta_2 - \theta_1) + c(\dot{\theta}_2 - \dot{\theta}_1))}\right)} \\
 \tau_{fA2} &= \frac{\left(k(\theta_2 - \theta_1) + c(\dot{\theta}_2 - \dot{\theta}_1)\right)}{\left(1 + e^{-2r(\theta_2 - \theta_1)}\right) \left(1 + e^{-2r(k(\theta_2 - \theta_1) + c(\dot{\theta}_2 - \dot{\theta}_1))}\right)}
 \end{aligned}$$

Appendix B. CASE B, COMPONENTS OF THE MATRICES  $M_B$  AND  $C_B$  AND THE VECTOR  $G_B$

$$\begin{aligned}
 m_{B11} &= 0, m_{B12} = 0, m_{B13} = \frac{1}{2}l_1(m_1 + 2m_2) \cos \theta_1 \\
 m_{B14} &= \frac{1}{2}m_2l_2 \cos \theta_2, m_{B21} = 0, m_{B22} = m_1 + m_2 \\
 m_{B23} &= \frac{1}{2}l_1(m_1 + 2m_2) \sin \theta_1, m_{B24} = \frac{1}{2}m_2l_2 \sin \theta_2 \\
 m_{B31} &= \frac{1}{2}l_1(m_1 + 2m_2) \cos \theta_1, m_{B32} = \frac{1}{2}l_1(m_1 + 2m_2) \sin \theta_1 \\
 m_{B33} &= \frac{1}{4}m_1l_1^2 + \bar{I}_1 + m_2l_1^2, m_{B34} = \frac{1}{2}m_2l_1l_2 \cos(\theta_1 - \theta_2) \\
 m_{B41} &= \frac{1}{2}m_2l_2 \cos \theta_2, m_{B42} = \frac{1}{2}m_2l_2 \sin \theta_2 \\
 m_{B43} &= \frac{1}{2}m_2l_1l_2 \cos(\theta_1 - \theta_2), m_{B44} = \frac{1}{4}m_2l_2^2 + \bar{I}_2 \\
 c_{B11} &= 0, c_{B12} = 0, c_{B13} = -\frac{1}{2}(l_1(m_1 + 2m_2) \sin \theta_1) \dot{\theta}_1 \\
 c_{B14} &= -\frac{1}{2}(m_2l_2 \sin \theta_2) \dot{\theta}_2, c_{B21} = 0, c_{B22} = 0 \\
 c_{B23} &= \frac{1}{2}l_1((m_1 + 2m_2) \cos \theta_1) \dot{\theta}_1, c_{B24} = \frac{1}{2}(m_2l_2 \cos \theta_2) \dot{\theta}_2 \\
 c_{B31} &= 0, c_{B32} = 0, c_{B33} = 0, c_{B34} = \frac{1}{2}(m_2l_1l_2 \sin(\theta_1 - \theta_2)) \dot{\theta}_2 \\
 c_{B41} &= 0, c_{B42} = 0, c_{B43} = -\frac{1}{2}(m_2l_1l_2 \sin(\theta_1 - \theta_2)) \dot{\theta}_1, c_{B44} = 0 \\
 g_{B1} &= \frac{1}{2}m_2l_2 \cos \theta_2, g_{B2} = m_1g + m_2g, \\
 g_{B3} &= \frac{1}{2}(m_1 + 2m_2)gl_1 \sin \theta_1, g_{B4} = \frac{1}{2}m_2gl_2 \sin \theta_2
 \end{aligned}$$